Supplement of Atmos. Chem. Phys., 22, 12769–12787, 2022
https://doi.org/10.5194/acp-22-12769-2022-supplement

Atmospheric Chemistry and Physics
Open Access
EGU

Supplement of

Hybrid water adsorption and solubility partitioning for aerosol hygroscopicity and droplet growth

Kanishk Gohil et al.

Correspondence to: Akua Asa-Awuku (asaawuku@umd.edu)

S1. CCN counter (CCNC) calibration

CCNC calibration was performed using the $(NH_4)_2SO_4$ aerosol. Dry $(NH_4)_2SO_4$ were subjected to supersaturated conditions when passing through the CCNC column. The set supersaturation inside the CCNC column depends on the axial temperature gradient for specified flow and pressure gradient. Ideally, the temperature gradient inside the CCNC column is assumed to stay constant. That is, if the CCNC parameters are maintained constant, then the temperature gradient and hence the supersaturation across the CCNC column must stay constant. However, in practice there are fluctuations in the CCNC parameters and so there are deviations in the "true" instrument supersaturation relative to the set supersaturation displayed on the CCNC software interface. These deviations can be resolved by calibrating the CCNC supersaturation using a compound like $(NH_4)_2SO_4$. $(NH_4)_2SO_4$ is one of most well-understood and well-characterized aerosol compounds that is widely used for CCNC calibration. Calibration was performed by following the procedure described by Rose et al. (2008).

Table S1. Sample CCN Counter (CCNC) calibration data using $(NH_4)_2SO_4$

Supersaturation Setting (%)	Calibrated Supersaturation (%)	Critical Dry Diameter (nm)
0.2	0.215	75.6 ± 2
0.4	0.402	52.3 ± 0.6
0.6	0.586	41.2 ± 0.4
0.8	0.771	34.7 ± 0.7
1.0	0.957	29.6 ± 0.6
1.2	1.125	26.1 ± 0.9
1.4	1.357	23.1 ± 1.1
1.6	1.546	$21.2 \pm 1.$

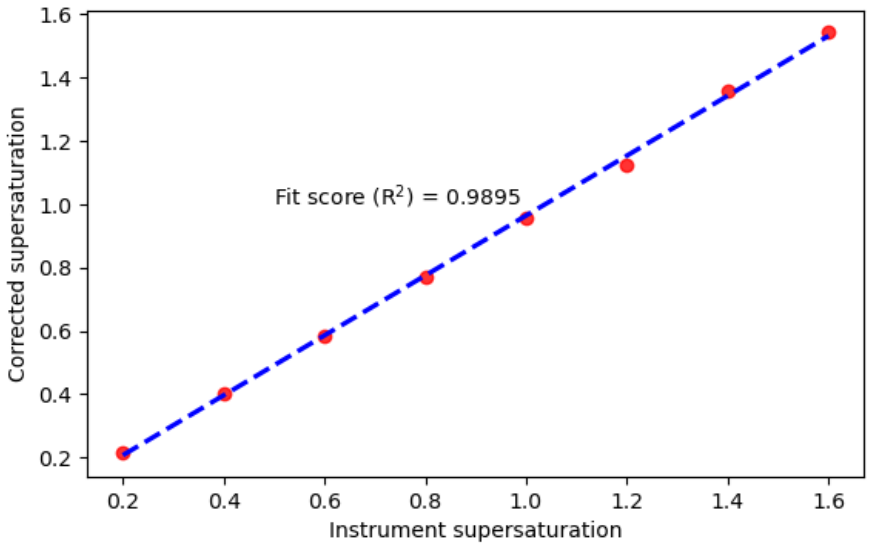

Figure S1. CCNC calibration curve generated using the ammonium sulfate activation data provided in Table S1. This curve was used to calibrate the CCNC supersaturations at which AAA data was collected.

S2. Single hygroscopicity parameter (κ_{HAM}) formulation from Hybrid Activity Model (HAM)

HAM is mathematically expressed as,

$$S = a_{w,HAM} \cdot \exp\left(\frac{A}{D_p}\right) \quad \text{(S.1)}$$

where S is supersaturation, $a_{w,HAM}$ is the water activity derived by combining features from FHH adsorption theory and Kohler theory, D_p is the intermediate diameter of the droplet, and A is a constant which is given as,

$$A = \frac{4M_w\sigma_w}{RT\rho_w} \quad \text{(S.2)}$$

Where M_w is the molecular weight of water, R is the gas constant, T is the temperature and ρ_w is the density of water. σ_w is the surface tension of the droplet and is assumed to be the same as that of pure water.

The development of $a_{w,HAM}$ has been described in detail in the main literature (Section 3.3) explaining that $a_{w,HAM} = X_w \cdot \exp(-A_{FHH}\theta^{-B_{FHH}})$. $a_{w,HAM}$ is then equated with the parameterization defined in terms of the single hygroscopicity parameter (κ) which is expressed as,

$$a_{w,HAM} = X_w \cdot \exp(-A_{FHH} \cdot \theta^{-B_{FHH}}) = \left[1 + \kappa \cdot \frac{v_s}{v_w}\right]^{-1} \quad \text{(S.3)}$$

Rearranging Eq. (S.3) provides the expression for κ_{HAM} as,

$$\kappa_{HAM} = \frac{6\theta D_w}{D_d}\left(\frac{1}{X_w \cdot \exp(-A_{FHH}\theta^{-B_{FHH}})} - 1\right) \quad \text{(S.4)}$$

Eq. (S.4) is the function of the measured D_d and D_p derived corresponding to the point of activation. Eq. (S.4) can be further simplified using Eq. (S.3). The exponential on the right-hand side of Eq. (S.3) can be simplified using the Taylor's series expansion for an exponential function such that,

$$\exp(-A_{FHH}\theta^{-B\_FHH}) = 1 + (-A_{FHH}\theta^{-B\_FHH}) + (-A_{FHH}\theta^{-B_{FHH}})^2 + \cdots \quad \text{(S.5)}$$

Since $-A_{FHH}\theta^{-B_{FHH}} \ll 1$, (S.5) can be restated as,

$$\exp(-A_{FHH}\theta^{-B\_FHH}) \approx 1 + (-A_{FHH}\theta^{-B\_FHH}) \quad \text{(S.6)}$$

The X_w term on the right-hand side of Eq. (S.3) is expressed depending on the ongoing phase of the droplet formation/growth. The phases of droplet formation/growth are described in detail in the main literature (Section 3.3). The left-hand side of Eq. (S.3) can be simplified under the assumption that $v_w \gg v_s$,

$$\left[1+\kappa\cdot\frac{v_s}{v_w}\right]^{-1}\approx 1-\kappa\cdot\frac{v_s}{v_w} \tag{S.7}$$

Combining Eq. (S.6) and Eq. (S.7) provides a simplified theoretical expression for κ_{HAM},

$$\kappa_{HAM,s}=\frac{6\Theta_c D_w}{D_{dry}}\cdot\left(1-X_w\left(1-A_{FHH}\cdot\Theta_c^{-B_{FHH}}\right)\right) \tag{S.8}$$

Eq. (S.8) contains critical θ defined as the point of activation such that $\theta=\theta_c$. θ_c is determined by taking the first derivative of Eq. (S.1) and equating it to 0 to represent the point of activation such that,

$$\frac{dS}{dD_p}=\frac{d}{dD_p}\left(X_w\cdot\exp\left(-A_{FHH}\cdot\left[\frac{D_p-D_d}{2\cdot D_w}\right]^{-B_{FHH}}\right)\cdot\exp\left(\frac{A}{D}\right)\right)=0 \tag{S.9}$$

$$1-\frac{2\theta_c D_w}{D_d}=\left(\frac{2AD_w}{A_{FHH}B_{FHH}D_d^2}\right)^{1/2}\theta_c^{\frac{B_{FHH}+1}{2}} \tag{S.10}$$

Solving Eq. (S9) and (S10) under different conditions prescribed by X_w (depending on the phase of droplet growth) will yield the appropriate θ_c to then subsequently parameterize κ_{HAM}.

S3. CCN data for pure and internally mixed aromatic acid samples

Figure S2 shows exemplary size-resolved activation ratios derived using the CCN measurements of the pure and internally mixed AAA samples. The activation ratio data are shown with respect to the electrical mobility diameter of the particles which were converted to their respective volume equivalent diameters using their shape factor measurements (shown in Section S4).

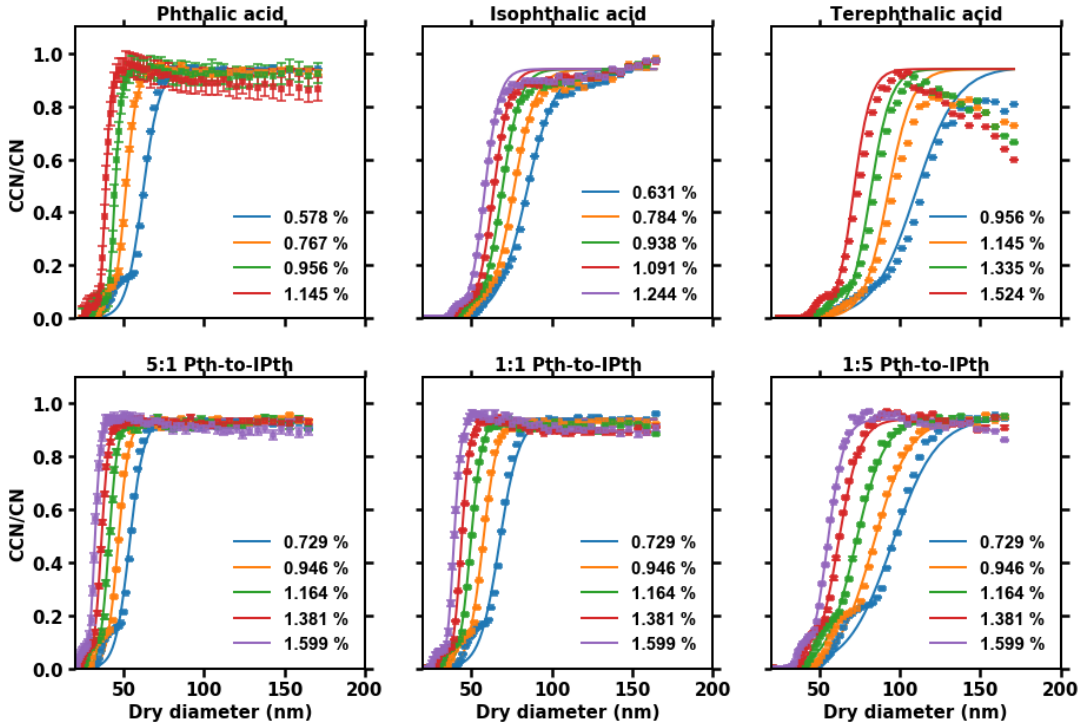

Figure S2. Size-resolved activation ratio of pure and internally mixed AAA samples from a typical DMA-based CCN setup. The activation ratio are overlayed with their corresponding sigmoidal fits which were used to determine the critical diameters $(D_{dry,c})$ at the respective supersaturations provided in the legend.

S4. Shape factor experiments

S4.1. Experimental setup

Shape factor measurements were conducted using a setup based on the Aerodynamic Aerosol Classifier (AAC) instrument. The experimental setup has been explained in detail in the literature (ref). Briefly explained here – the AAC is used to size-select particles of a specific aerodynamic diameter from the incoming polydisperse population. The size-selected aerosols are then passed through a Scanning Mobility Particle Sizer (SMPS) setup to generate a distribution with respect to electrical mobility diameter. The geometric mean of the number distribution is considered as the mobility size measurement corresponding to the aerodynamic diameter. The mobility diameter and aerodynamic diameter are then used to estimate the volume equivalent diameter and dynamic shape factor using a set of coupled equations (Section 3.3, Tavakoli and Olfert (2014)).

S4.2. Measured data for aromatic acid aerosols (AAAs)

The exemplary shape factor data of pure AAA samples are shown with respect to the aerodynamic diameter of the particles (Fig. S3). The aerodynamic diameters chosen here ranged from ~100 to 200 nm. This range of aerodynamic diameters corresponds to the electrical mobility diameters ranging from ~50 to120 nm. This is similar to the range in which the measure critical dry diameters $\left(D_{dry,c}\right)$ of pure and internally mixed samples were observed.

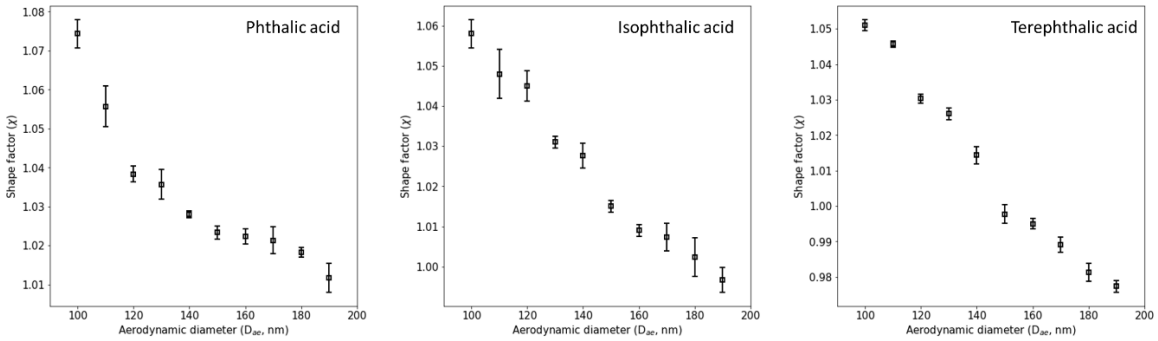

Figure S3. Dynamic shape factor measurements for pure phthalic acid (PTA), isophthalic acid (IPTA) and terephthalic acid (TPTA). The shape factor data is plotted against the aerodynamic diameter of the particles and can be converted their respective mobility diameters or volume equivalent diameter using Eq. (S11) or (S12), respectively. Since most of the shape factor values lie in close range to 1 (~5% of 1; or close to 1.05), it can be assumed that AAA particles studied in this work are spherical in shape.

S5. Solubility-limited Köhler theory application to pure and internally mixed aromatic acids

Köhler theory traditionally accounts for the intrinsic hygroscopicity of the compounds that depends only on the solute and solvent (water) properties (Section 3.1; Section 4.1 for results). For compounds that are not completely water soluble, traditional Köhler theory can be modified by explicitly accounting for the aqueous solubility of the compound.

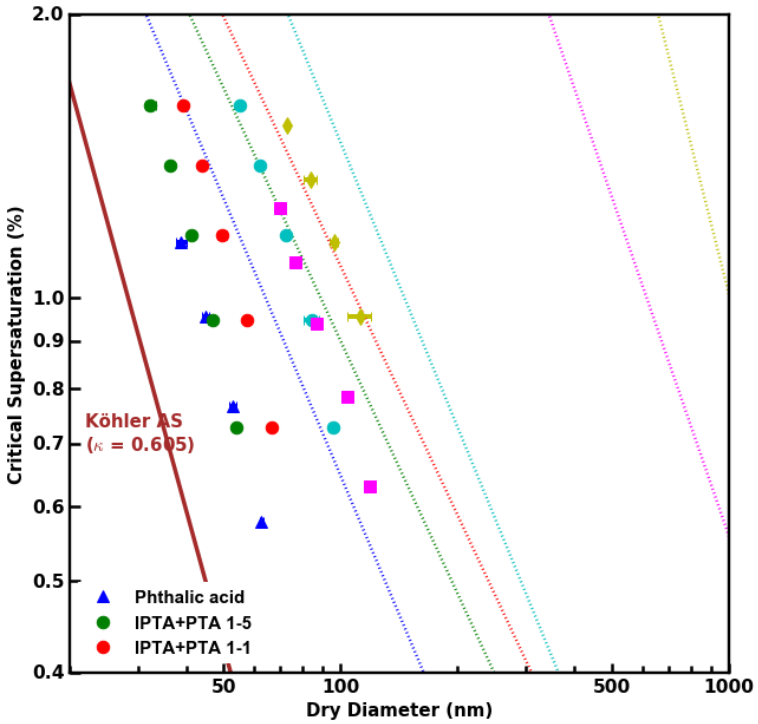

Figure S4. CCN measurements of pure and internally mixed AAA samples from a typical DMA-based CCN setup. The activation measurements are overlayed with solubility limited Köhler theory fits line which were derived using the apparent hygroscopicity parameter $(\kappa_{apparent})$ of the pure and internally mixed samples.

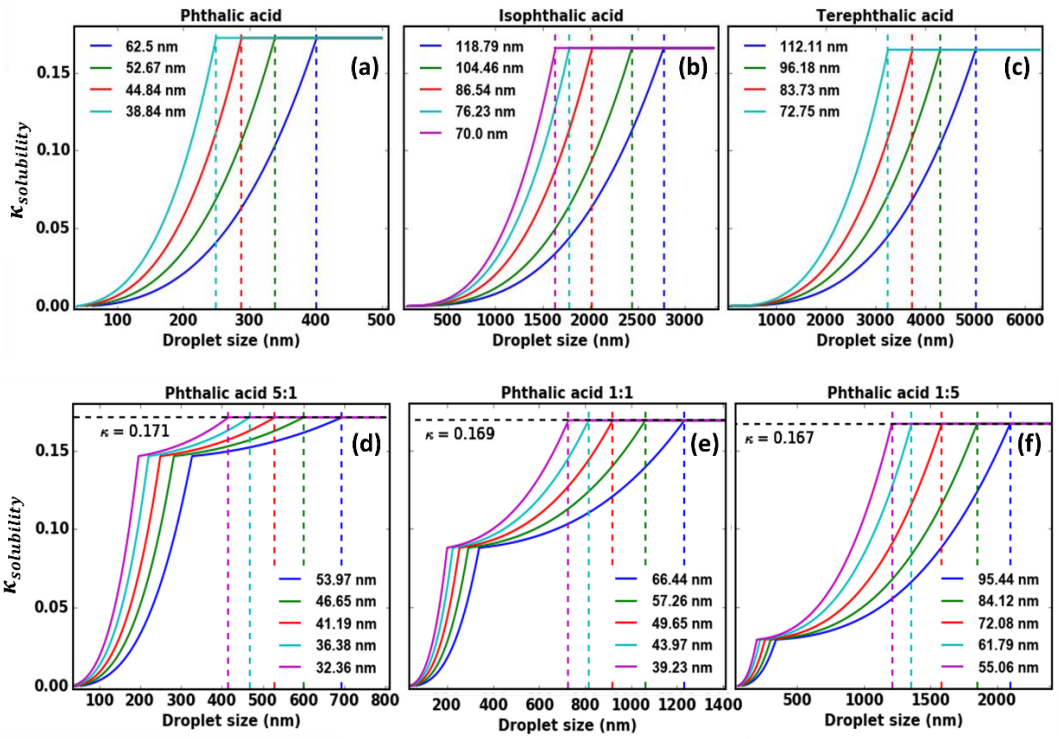

Figure S5. $\kappa_{apparent}$ plotted against droplet size for pure and internally mixed AAA samples. $\kappa_{apparent}$ was determined using Eq. (11) described in detail in Section 3.1.

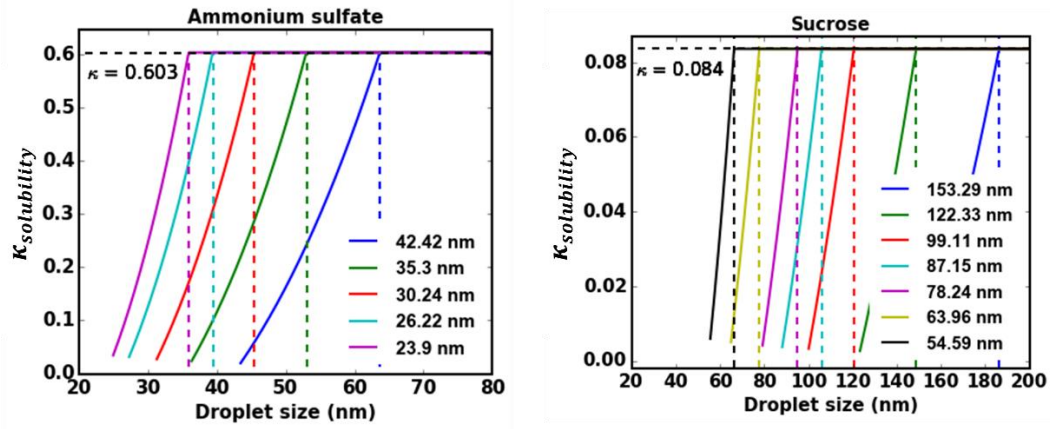

Figure S6. $\kappa_{apparent}$ plotted against droplet size for high solubility compound – ammonium sulfate (AS) and sucrose, respectively. $\kappa_{apparent}$ was determined using Eq. (11) described in detail in Section 3.1. It can be observed that the droplet sizes that needs to be attained at $\kappa_{apparent}$ for highly soluble compounds is significantly lower than those for AAAs (described in detail in Section 4.1). This is an important consideration for the assumption that AS and sucrose almost instantly dissolve in water, hence making traditional KT applicable for analysis.